Cumhuriyet Sci. J., 43(1) (2022) 45-52
DOI: https://doi.org/10.17776/csj.1004338

Cumhuriyet Science Journal

| csj.cumhuriyet.edu.tr | Founded: 2002 ISSN: 2587-2680 e-ISSN: 2587-246X Publisher: Sivas Cumhuriyet University

CT-DNA/BSA Binding Studies of Thiosemicarbazone-Derivated Zn(II) Complex

Asuman Uçar[1,a,*], Mükerrem Fındık[2,b], Emine Güler Akgemci[3,c]

[1] *Department of Science Education, Education Faculty, Agri Ibrahim Cecen University, Ağrı, Turkey*
[2] *Department of Chemistry Education, Research Laboratory, A.K. Education Faculty, Necmettin Erbakan University, Konya, Turkey*
[3] *Department of Chemistry Education, A.K. Education Faculty, University, , Necmettin Erbakan University, Konya, Turkey*
**Corresponding author*

Research Article

History
Received: 04/10/2021
Accepted: 07/02/2022

ABSTRACT

Zn(II) complex of 2-hydroxy-5-methoxyacetophenone thiosemicarbazone { $Zn(HMAT)_2$} was synthesized and characterized by ^1H NMR, UV–Vis and FT-IR spectroscopies. Further, X-ray powder diffraction (XRD) analysis of $Zn(HMAT)_2$ was carried out to point out the complexation. The binding affinities of $Zn(HMAT)_2$ with calf thymus DNA (CT-DNA) have been studied by using fluorescence and absorption titration technics. In addition, bovine serum albumin (BSA) binding studies were recorded by fluorescence and UV–Vis spectroscopy. $Zn(HMAT)_2$ is a strong binders of CT-DNA with binding constant (K_b) 3.65×10^7 M^{-1}. The binding parameters K_{SV} (for EB), K_q (for BSA) and K_b (for BSA) were determined as 8.2×10^7 M^{-1}, 1.8×10^{14} M^{-1} s^{-1} and 2×10^7 M^{-1} respectively.

Keywords: DNA, Thiosemicarbazone, Zn(II) complex, Bovine serum albumin binding.

[a] asucar340@gmail.com https://orcid.org/0000-0003-2674-3120
[b] mmukerremm@gmail.com https://orcid.org/0000-0002-9441-0814
[c] egakgemci@gmail.com https://orcid.org/0000-0002-9744-1931

Introduction

DNA is the fundamental intracellular target in drug design (1). Combination of DNA and small molecules can give rise to cell death and cancer cells DNA damage (2). However, transition metal complexes are being studied by researchers for DNA binding experiments due to their regulators of gene expression, potential use as drugs and DNA structural probes (3-4). In previous studies, it was reported that, compounds with sulfur content show high DNA/protein binding/cleaving (5-7). Thiosemicarbazones present pharmacological properties due to their C=S and NH moiety for chelating with metal center (8). Metal complexes of thiosemicarbazones exhibit more biological activity than their ligands (9). In previous studies, DNA binding assays, anticancer activity, antimicrobial and cytotoxicity evaluation of some thiosemicarbazones zinc complexes have been investigated (10-12). Zinc differs from other transition metals due to some properties such as the malleable coordination geometry, remarkably high bioavailability and the role as a Lewis acid (13). In the presence of zinc metal, proteins' conformation changes rapidly to carry out biological reactions due to their flexible coordination geometry (14). Understanding the interaction between proteins and metal complexes cause the development of new drugs (15). Bovine serum albumin (BSA), which is the protein in the blood, take place in many researches due to its low cost (16), structural homology to human serum albumin and stability (17).

Synthesis method of 2-hydroxy-5-methoxyacetophenone thiosemicarbazone based Zn(II) complex and its application studies such as evaluation of anticancer activity in breast cancer cell lines, carbonic anhydrase inhibition and microbiological analysis results were included in our previous study (18,19). In addition, the investigation of binding properties CT-DNA and BSA with the compound have been presented in this article.

Materials and Methods

Apparatus

Thiosemicarbazide, 2-hydroxy-5-methoxyacetophenone, DMF (N,N-Dimethylformamide) EtOH (Ethyl alcohol), H_2SO_4 (Sulfuric acid), CT-DNA (Deoxyribonucleic acid from calf thymus) and Trizma base (for Tris/HCl buffer) were obtained from Sigma–Aldrich and Merck. ^1H NMR spectrum was monitored by A Bruker AC 400 (400 MHz) NMR spectrometer. FT-IR spectrum was carried out by using Attenuated Total Reflection-Fourier Transformed Infrared (ATR-FTIR) spectrometer (Perkin Elmer 100). UV–Vis and fluorescence spectra were monitored by Shimadzu UV-1800 double beam spectrophotometer and PTI Quantamaster 400 Fluorometer spectrophotometer, respectively. XRD measurement was recorded using Bruker axis diffractometer (Bruker D8 ADVANCE).

Synthesis of $Zn(HMAT)_2$

Zn(HMAT)$_2$ was synthesized (Scheme 1) according to our previous article (18,19). The possible structure of the complex is given in Scheme 1 (20,21).

$Zn(HMAT)_2$: Yellow crystals, yield 72.5%; mp: 189-191°C Anal. Calcd. $C_{20}H_{22}N_6O_4S_2Zn$: H, 4.11; N, 15.56; C, 44.49%. Found: H, 4.19; C, 45.03; N, 15.68%. FT-IR (cm^{-1}) υ: 585, 783, 1030, 1215, 1540, 3192, 3486. ^1H NMR (400 MHz, DMSO-d_6): δ (ppm): 2.35-3.78 (s, 3H, -CH_3), 6.84-6.93 (d, 2H, H_{Ar}), 7.24 (s, 2H, -NH_2).

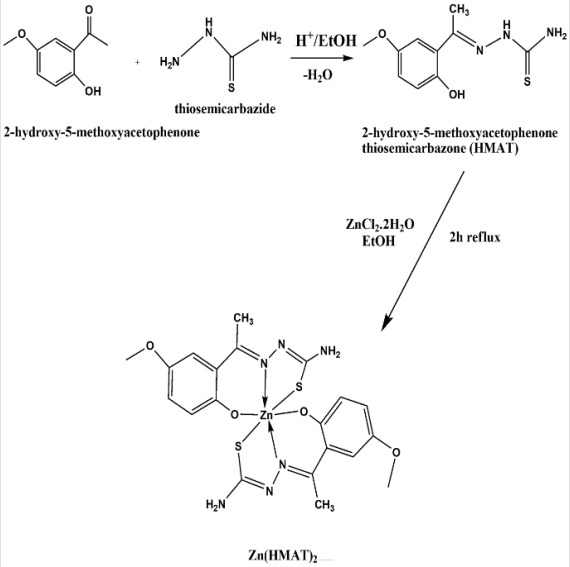

Scheme 1. Proposed structures of HMAT and Zn(HMAT)2

Dna Binding Experiments

The interactions of $Zn(HMAT)_2$ with CT-DNA were explored using UV–visible absorption titration experiments. All titration experiments of $Zn(HMAT)_2$ with CT-DNA were investigated in a pH 7.2 Tris/HCl buffer (5 mM Tris/50 mM NaCl). The emission spectra were recorded with the compound (20 µM in DMF), during which the concentration of CT-DNA (2-5.5 µM) was gradually increased.

Competitive Ethidium Bromide-Dna Binding Fluorescence Measurement

Displacement experiments of EB have been monitored fluorometrically upon gradual addition of $Zn(HMAT)_2$ (1-4 µM) to the aqueous solution of EB (10 µM) bound CT-DNA (10 µM) in Tris-HCl buffer (5 mM Tris/50 mM NaCl, pH 7.2).

Protein Binding Studies

The absorbance measurements were monitored of 10 µM BSA in phosphate-buffered saline (PBS) and BSA with $Zn(HMAT)_2$ (4 µM in DMF). The interaction of $Zn(HMAT)_2$ with BSA was investigated by using fluorescence spectra. The fluorometric measurements were recorded by gradual addition of 0-1 µM $Zn(HMAT)_2$ to 2 mL, 2 µM BSA with PBS at pH 7.5.

Results and Discussion

Spectroscopic Studies

The ^1H NMR spectrum of $Zn(HMAT)_2$ was recorded in DMSO-d_6 (Figure 1). A multiple signal for aromatic protons were observed around 6.93-6.84 ppm (22). A singlet was appeared at 7.24, 3.78 and 2.35 ppm was attributed to proton signal of the $–NH_2$, CH_3 (methoxy group) and $-CH_3$ (azomethine group), respectively (22-25).

The FT-IR spectrum of $Zn(HMAT)_2$ (Figure 2) displayed stretching frequency bands for the υ(C=N) at 1540 cm^{-1} (26). The bands attributed to υ(Zn-N) vibration was found at 585 cm^{-1} (27). υ(N-H) stretching frequencies of the NH_2 was observed at 3486 cm^{-1} (28). υ(C–S) vibration at 783 cm^{-1} was proved the coordination of the NH–C=S group [22]. The band at 1215 cm^{-1} was appeared due to the υ(N-C-S) vibration (29).

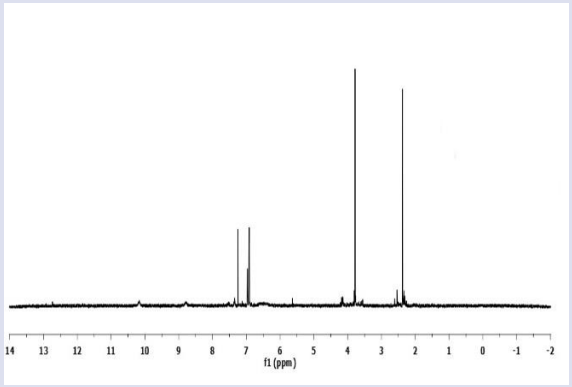

Figure 1. ^1H NMR spectrum of $Zn(HMAT)_2$.

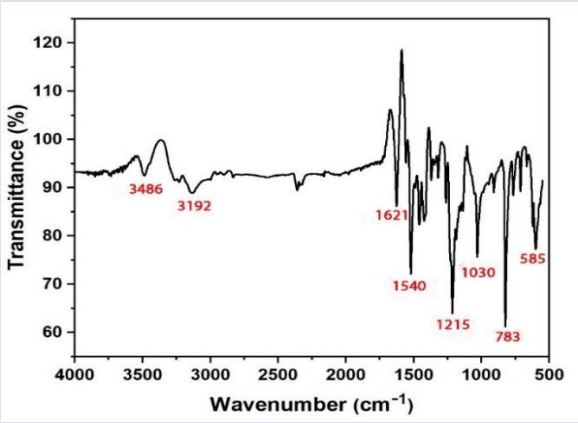

Figure 2. FT-IR spectrum of $Zn(HMAT)_2$.

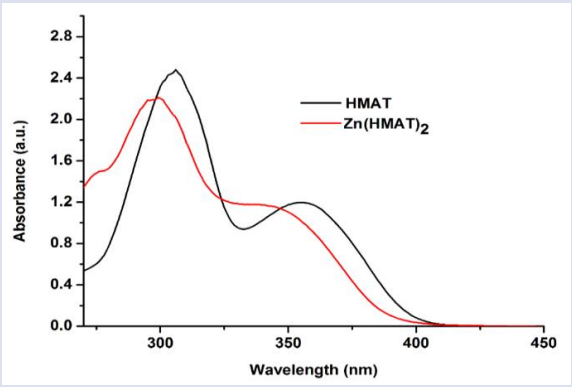

Figure 3. UV-Vis spectra of HMAT and $Zn(HMAT)_2$.

UV-Vis spectra of HMAT and $Zn(HMAT)_2$ (in DMF) was presented in Figure 3. In the UV-Vis spectrum of HMAT, the band at 305 nm belongs to azomethine π→π* transitions, whereas the absorption at 355 nm corresponds to thioamide n→π* transitions (19). After the complexation, the first band associated with the carbonyl and azomethine group was observed at 296 nm due to π→π* transitions (30). The intraligand n→π* transition was assigned to band at 346 nm (31). Transformation of the C=S bond to the C-S form due to complexation caused the shift of the bands (32). By comparing the frequency of

HMAT and the corresponding the Zn complex, the electronic transitions of π→π* are shifted to a lower value due to the formation of the complex and coordination of the ligand to the metal (18).

Powder XRD Analysis

The powder X-ray diffraction pattern of $Zn(HMAT)_2$ (Figure 4) was monitored over the range 5-80 (2θ). The diffraction peak at 2Θ=24.06 may have been caused by the bond of Zn-S (33,34). Observing the sharp crystalline peaks arise the crystalline behavior of the samples (35).

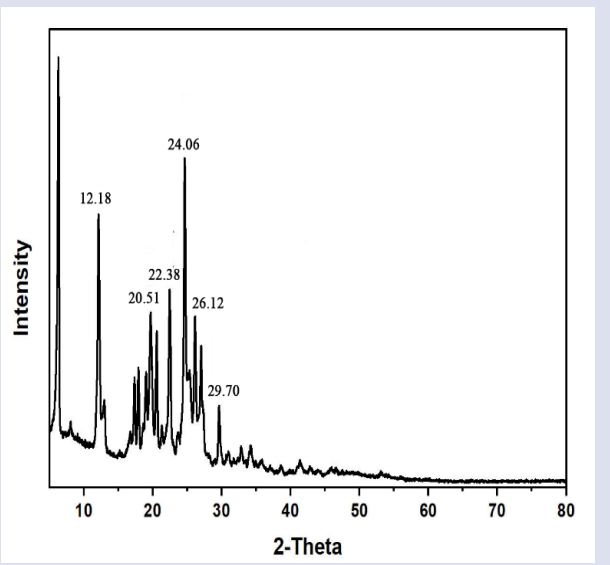

Figure 4. X-ray diffraction (XRD) spectrum of $Zn(HMAT)_2$.

DNA Binding Studies

UV absorption spectra of DNA

UV-visible absorption spectra of complex (20 µM) with increasing ratios of CT-DNA (2−5.5 µM; Tris-HCl 5 mM/NaCl 50 mM, pH: 7.2) were measured to observe the binding interaction (Figure 5A). After increasing the amount of CT-DNA to the complex, the spectrum showed a hypochromism of about 8%, 21% at 275, 344 nm and showed a hypochromism of about 13% with a blue shift of 4 nm at 296 nm. According to the results obtained, the binding to CT-DNA was confirmed from the absorption changes of the complex. The amount of binding interaction between $Zn(HMAT)_2$ and CT-DNA was described using the binding constant K_b, which is calculated from the Eq. (1).

$$\frac{[DNA]}{(\varepsilon_a-\varepsilon_f)} = \frac{[DNA]}{(\varepsilon_b-\varepsilon_f)} + \frac{1}{K_b(\varepsilon_b-\varepsilon_f)} \quad (1)$$

Where [DNA] is the concentration of CT-DNA, ε_f, ε_a, and ε_b correspond to the extinction coefficient for the free complex, A_{obsd}/[complex] and the extinction coefficient for the complex in the fully bound form, respectively. K_b was found by calculating the ratio of slope/intercept in the linear plot of [DNA]/(ε_a−ε_f) vs [DNA] (Figure 5B). The binding constant (K_b) value for the interaction of the complex with CT-DNA was found as 3.65×10^7 M^{-1}. The UV-Vis spectroscopy method provides important data about interaction type on absorbance changes and shift in wavelength in the interaction of small molecules with DNA. Hypochromism with or without a red or blue shift is typically the product of a compound binding to DNA through intercalation. The observed hypochromism with blue shift verified the complex's interaction (36-38).

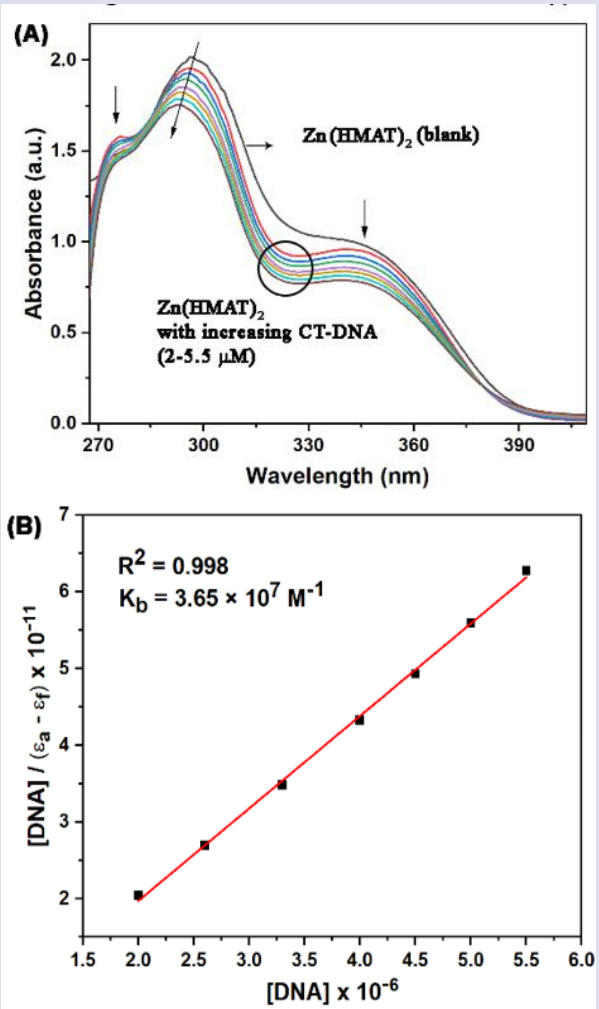

Figure 5. A) Absorption spectrum of the complex with increasing CT-DNA. B) Plot of [DNA]/(ε_a−ε_f) versus [DNA] for the titration of the complex with CT-DNA.

Ethidium bromide (EB) displacement

EB is a dye which binds to DNA through intercalation. EB exhibits increased fluorescence intensity after addition of DNA because of the strong intercalation between DNA. EB binding to the DNA by intercalation is cause competition with EB and affect the combination between EB and DNA, giving rise to a decrease in fluorescence intensity (39,40). The study was carried out by titration of the complex varying from 1 to 4 µM into 10 µM CT-DNA and 10 µM EB solution. After addition of each aliquot, 540 nm was used as excitation wavelength for the CT-DNA-EB with $Zn(HMAT)_2$ (in the range of 550 nm and 780 nm for emission spectra). The fluorescence spectra of the CT-DNA –EB and CT-DNA–EB with $Zn(HMAT)_2$ (Figure 6a) show the decreasing fluorescence intensity of CT-DNA-EB in each addition with increasing amounts of complex. This result indicated that complex was

able to replace EB in the CT-DNA helix. Thus, this result proves that $Zn(HMAT)_2$ binds to CT-DNA via intercalative binding mode. The quenching efficiency for $Zn(HMAT)_2$ was evaluated by the Stern–Volmer constant K_{SV},

$$F^o/F = 1 + K_{SV}\,[Q] \qquad (2)$$

where F/F^0, K_{SV}, [Q] are the fluorescence intensities in the presence/absence of the complex, the linear Stern–Volmer quenching constant and concentration of the complex, respectively. The K_{SV} value calculated from the ratio of slope/intercept in the linear plot of [Q] vs F^0/F and is found to be 8.2×10^7 M^{-1} (Figure 6b).

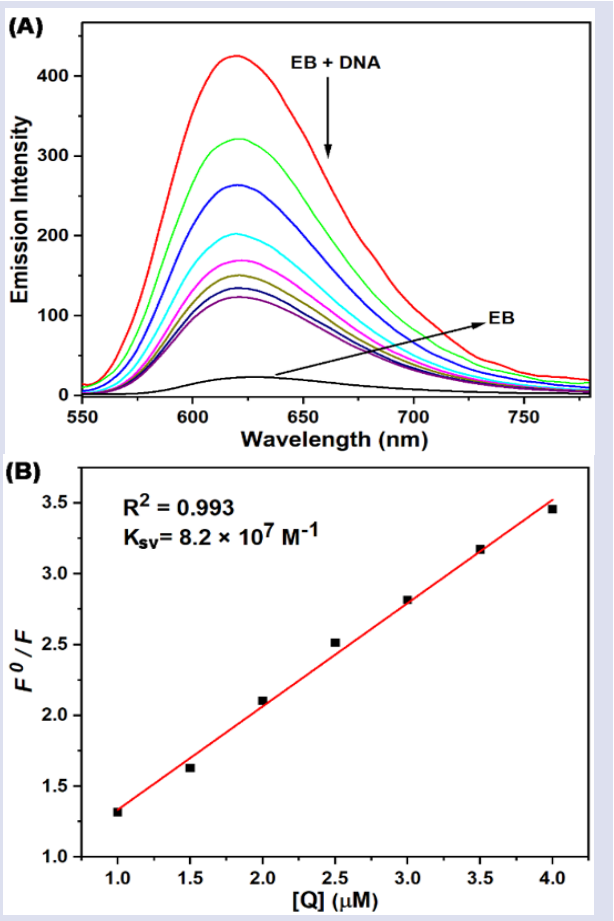

Figure 6. A) Fluorescence quenching curves with increasing complex to DNA/EB. Conditions: [CT-DNA] = 10 µM, [EB] = 10 µM, [complex] = 1–4 µM. B) Stern–Volmer plot of fluorescence titrations of the complex with CT-DNA.

BSA binding studies

Fluorescence quenching of BSA.

Fluorescence of the BSA is due to the fluorophore groups in its structure such as phenylalanine, tyrosine and tryptophan. When any compound interacts with BSA, fluorescence intensity quenches (37,41).

Tryptophan fluorescence quenching study was used to indicate BSA-binding. In this experiment, varied mole ratio of $Zn(HMAT)_2$ solutions to 2 µM BSA in PBS buffer solution were prepared (pH:7.5). The fluorescence spectra were monitored with emission at 341 nm whereas excitation wavelength is 280 nm. The additions of different concentration of $Zn(HMAT)_2$ (0–1 µM) solutions to BSA were decrease its fluorescence intensity and a blue shift (341-337 nm) was noticed. The resulting emission behaviour is shown in Figure 7A. The emission spectra demonstrated a definite interaction between BSA and $Zn(HMAT)_2$. The extent of fluorescence quenching of BSA with the gradual addition of the complex was interpreted by using the Stern–Volmer equation (3).

$$\frac{F_0}{F} = 1 + K_q\tau_0[Q] = 1 + K_{SV}[Q] \qquad (3)$$

Where F/F_0, K_q, [Q] and τ_0 the fluorescence intensities in the presence/absence of the complex, the bimolecular quenching rate constant, the concentration of the complex and the average lifetime (10^{-8} s) of protein without complex, respectively. K_{SV} is the Stern–Volmer quenching constant and is equal to $K_q\tau_0$. The linear Stern-Volmer plot in Figure 7b indicated that equation (3) is useable for the present system and the numerical values of K_{SV} and K_q were equal to 1.8×10^6 M^{-1} and 1.8×10^{14} M^{-1} s^{-1}, respectively. The calculated K_q value is larger than the limiting diffusion constant K_{dif} (2.0×10^{10} M^{-1} s^1) of the biomolecules (42) which indicated that fuorescence quenching is caused by interaction of BSA with $Zn(HMAT)_2$ depending on static quenching mechanism. (43).

Constant K_b and the number of binding site *n* were calculated by using following Scatchard equation (4).

$$\log[(F_0 - F)/F] = log\,K_b + nlog[Q] \qquad (4)$$

Where F/F_0, K_b and *n* are the fluorescence intensity in the presence/absence of the complex, the binding constant of complex with BSA and the number of binding sites. The K_b and *n* were calculated from the ratio of slope/intercept in the linear plot of $\log[(F_0\text{-}F)/F]$ *vs* log[Q] and was found to be 2×10^7 M^{-1} and *n* = 0.998 (Figure 7C). Existence of only one binding site on BSA for complex can be provided with the value for the binding site *n* which is close to 1. The values of K_q and K_b clearly evidence a strong interaction between BSA and $Zn(HMAT)_2$. When the related publications are examined, the large K_b and K_q values indicate that the strength of the interaction increases (44,45).

In Table 1, comparison of our work with other studies can be seen by observing the higher values K_b and K_q of $Zn(HMAT)_2$ indicating a stronger interaction.

Table 1. Comparison with other Zn complexes for Binding constant (Kb) and quenching constant (K_q) values of DNA and BSA

	DNA	BSA		
Complex	K_b (M^{-1})	K_b (M^{-1})	K_q(M^{-1})	Ref.
$Zn(HL)_2$	2.85×10^4	4.5×10^4	2.4×10^{13}	(46)
$Zn(L^{DiOMe}SN)_2$	1×10^5	2.03×10^5	1.67×10^{13}	(47)
$Tp^{py}ZnN_3$	6.79×10^4	5.37×10^4	1.19×10^5	(48)
$M(HL)_2](NO_3)_2$ (M:Zn)	$2.98 \pm 0.06 \times 10^6$	$\sim 4.68 \times 10^5$	6.31×10^{13}	(49)
ZnPc-4	1.58×10^5	no data	1.99×10^{13}	(50)
$Zn(H_2L)](NO_3)_2$	5.98×10^3	3.69×10^4	9.69×10^{10}	(51)
$Zn_2(L^4)(CH_3COO)$	2.7×10^3	2.4×10^6	$\sim 10^{13}$	(52)
Zn(II) complex	1.2×10^4	3.5×10^4	2.8×10^{12}	(53)
2,4-diiodo-6-((2-phenylaminoethylimino)methyl) phenol Zn Complex	1.2×10^4	2.14×10^4	1.66×10^5	(54)
$Zn(HMAT)_2$	3.65×10^7	2×10^7	1.8×10^{14}	This work

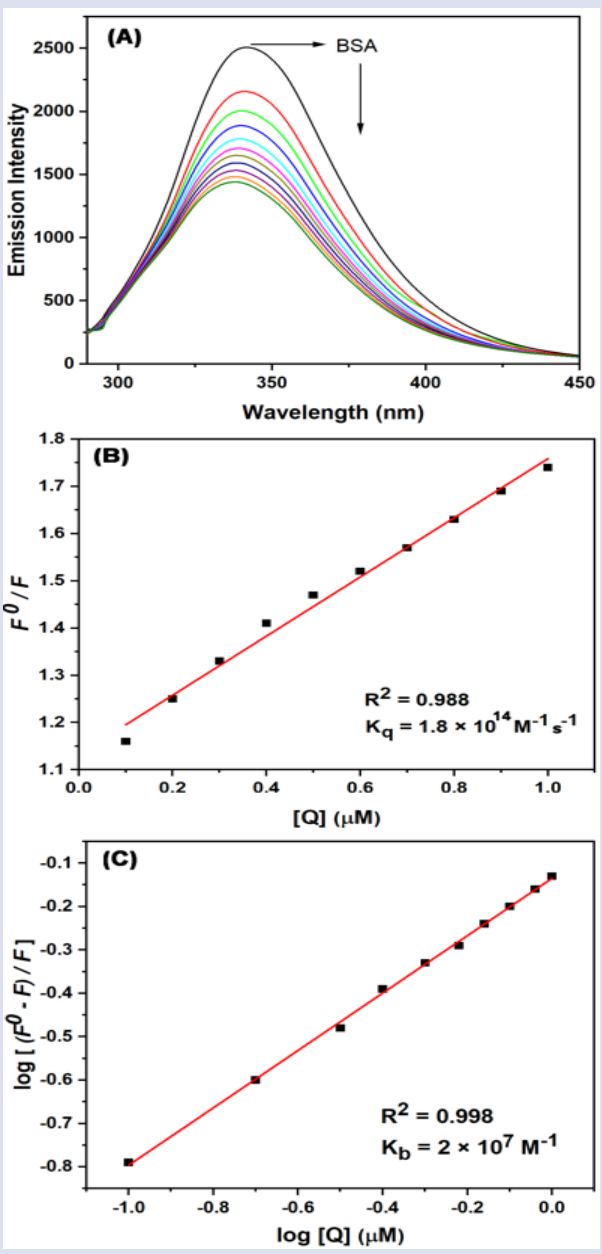

Figure 7. (A) Fluorescence quenching of BSA (1 μM; λ_{ex} = 280; λ_{em} = 341 nm) in the presence/absence of various concentrations of the complex (0–1 μM); (B) Stern–Volmer plot of the fluorescence titrations of the complex with BSA; (C) Scatchard plot of the fluorescence titrations of the complex with BSA.

UV absorption spectra of BSA.

The BSA solution exhibited a strong band around 278 nm for having the moieties such as phenylalanine, tyrosine and tryptophan. The absorption spectrum of the BSA solution and BSA- $Zn(HMAT)_2$ were given in Figure 8. The absorbance of BSA (10 μM) increased with 5 nm red shift with the addition of $Zn(HMAT)_2$ (4 μM), which indicated static quenching (36,55,56).

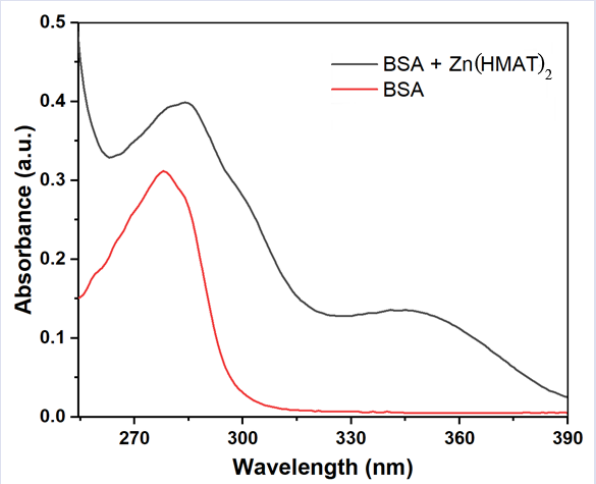

Figure 8. Absorption spectra of BSA (10 μM) and BSA with complex (4 μM).

Conclusion

In this study, synthesis and characterization by using spectroscopic methods (FT-IR, ^{1}H NMR, elemental analysis and UV–Vis spectroscopies) for zinc complex of 2-hydroxy-5-methoxyacetophenone thiosemicarbazone was reported. XRD spectrum of the complex also provided support for the analysis of the structure. BSA and DNA interactions abilities of the $Zn(HMAT)_2$ were analyzed by fluorescence and UV–Vis spectroscopy. The results showed that $Zn(HMAT)_2$ binds strongly with CT-DNA via intercalative mode with high binding constant. The results illustrated from absorption titrations as (K_b) 3.65×10^7 M^{-1} and ethidium bromide competitive studies as K_{SV} (for CT-DNA): 8.2×10^7 M^{-1} were obtained. Protein binding efficiency showed that $Zn(HMAT)_2$ interact with BSA by

acting as transporters of the complex (K_q: 1.8×10^{14} M^{-1} s^{-1} and K_b: 2×10^{7} M^{-1}). The reactivity towards BSA exhibited a static emission quenching by the complex. These findings may be useful in determining the mechanism of some Zn complexes' interactions with serum albumin and DNA.

Conflicts of Interest

The authors state that did not have conflict of interests

References

[1] Deng J.G., Li T., Su G., Qin Q.P., Liu Y., Gou Y., Co(III) complexes based on a-N-heterocyclic thiosemicarbazone ligands: DNA binding, DNA cleavage, and topoisomerase I/II inhibitory activity studies, *J. Mol. Struct.*, 1167 (2018) 33-43.

[2] Li V.S., Choi D., Wang Z., Jimenez L.S., Tang M.S., Kohn H., Role of the C-10 substituent in mitomycin C-1-DNA bonding, *J. Am. Chem. Soc.,* 118 (10) (1996) 2326–2331.

[3] Zuber G., Quada J.C., Hecht S.M., Sequence selective cleavage of a DNA octanucleotide by chlorinated bithiazoles and bleomycins, *J. Am. Chem. Soc.,* 120 (36) (1998) 9368–9369.

[4] Kalaiarasi G., Umadevi C., Shanmugapriya A., Kalaivani P., Dallemer F., Prabhakaran R., DNA(CT), protein (BSA) binding studies, anti-oxidant and cytotoxicity studies of new binuclear Ni(II) complexes containing 4(N)-substituted thiosemicarbazones, *Inorg. Chim. Acta,* 453 (2016) 547-558.

[5] Giannini F., Suss-Fink G., Furrer J., Efficient Oxidation of Cysteine and Glutathione Catalyzed by a Dinuclear Areneruthenium Trithiolato Anticancer Complex, *Inorg. Chem.,* 50 (21) (2011) 10552-10554.

[6] Suda Y., Arano A., Fukui Y., Koshida S., Wakao M., Nishimura T., Kusumoto S., Sobel M., Immobilization and Clustering of Structurally Defined Oligosaccharides for Sugar Chips: An Improved Method for Surface Plasmon Resonance Analysis of Protein−Carbohydrate Interactions, *Bioconjugate Chem.,* 17(5) (2006) 1125-1135.

[7] Mahon A.B., Arora P.S., Design, synthesis and protein-targeting properties of thioether-linked hydrogen bond surrogate helices, *Chem. Commun.,* 48 (2012) 1416-1418.

[8] shaq M., Taslimi P., Shafiq Z., Khana S., Salmas R.E., Zangeneh M.M., Saeed A., Zangeneh A., Sadeghian N., Asari A., Mohamad H., Synthesis, bioactivity and binding energy calculations of novel 3-ethoxysalicylaldehyde based thiosemicarbazone derivatives, *Bioorg. Chem.*, 100 (2020) 103924-103933.

[9] Zhang X., Li S., Yang L., Fan C., Synthesis, characterization of Ag(I), Pd(II) and Pt(II) complexes of a triazine-3-thione and their interactions with bovine serum albumin, *Spectrochim. Acta Part A*, 68(3) (2007) 763–770.

[10] Bessega T., Chaves O.A., Martins F.M., Acunha T.V., Back D.F., Iglesias B.A., Oliveira G.M., Coordination of Zn(II), Pd(II) and Pt(II) with ligands derived from diformylpyridine and thiosemicarbazide: Synthesis, structural characterization, DNA/BSA binding properties and molecular docking analysis, *Inorg. Chim. Acta*, 496 (2019) 119049-119058.

[11] Kumar S.M., Kesavan M.P., Kumar G.G.V., Sankarganesh M., Chakkaravarthi G., Rajagopal G., Rajesh J., New heteroleptic Zn(II) complexes of thiosemicarbazone and diimine Co-Ligands: Structural analysis and their biological impacts, *J. Mol. Struct.*, 1153 (2018) 1-11.

[12] Mathews N.A., Kurup M.R.P., In vitro biomolecular interaction studies and cytotoxic activities of copper(II) and zinc(II) complexes bearing ONS donor thiosemicarbazones, *Appl. Organomet. Chem.*, 35(1) (2020) 6056.

[13] Balakrishnan N., Haribabu J., Krishnan D.A., Swaminathan S., Mahendiran D., Bhuvanesh N.S.P., Karvembu R., Zinc(II) complexes of indole thiosemicarbazones: DNA/protein binding, molecular docking and in vitro cytotoxicity studies, *Polyhedron*, 170 (2019) 188–201.

[14] Haribabu J., Priyarega S., Bhuvanesh N.S.P., Karvembu R., Synthesis and molecular structure of the zinc(II) complex bearing an N, S donor ligand, *J. Struct. Chem.*, 61(1) (2020) 66-72.

[15] Zhang Y.Z., Zhou B., Liu Y.X., Zhou C.X., Ding X.L., Liu Y., Fluorescence Study on the Interaction of Bovine Serum Albumin with P-Aminoazobenzene, *J. Fluores.*, 18 (2008) 109-118.

[16] Zareia L., Asadi Z., Samolova E., Dusek M., Amirghofran Z., Pyrazolate as bridging ligand in stabilization of self-assemble Cu(II) Schiff base complexes: Synthesis, structural investigations, DNA/protein (BSA) binding and growth inhibitory effects on the MCF7, CT-26, MDA-MB-231 cell lines, *Inorg. Chim. Acta*, 509 (20201) 19674-119687.

[17] Ghosh K.S., Sen S., Sahoo B.K., Dasgupta S., A spectroscopic investigation into the interactions of 3′-O-carboxy esters of thymidine with bovine serum albumin, *Biopolymers*: *Orig. Res. Biomol.,* 91 (9) (2009) 737–744.

[18] Ucar A., Findik M., Kuzu M., Pehlivanoglu S., Sayin U., Sayin Z., Akgemci E.G., Cytotoxic effects, microbiological analysis and inhibitory properties on carbonic anhydrase isozyme activities of 2-hydroxy-5-methoxyacetophenone thiosemicarbazone and its Cu(II), Co(II), Zn(II) and Mn(II) complexes, *Res. Chem. Intermed.,* 47 (2021) 533-550.

[19] Akgemci E.G., Saf A.O., Tasdemir H.U., Türkkan E., Bingol H., Turan S.O., Akkiprik M., Spectrophotometric, voltammetric and cytotoxicity studies of 2-hydroxy-5-methoxyacetophenone thiosemicarbazone and its N(4)-substituted derivatives: A combined experimental–computational study, *Spectrochim. Acta Part A Mol. Biomol. Spectrosc.*, 136 (2015) 719-725.

[20] Kotian A., Kamat V., Naik K., Kokare D.G., Kumara K., Lokanath N.K., Revankar V.K., Hydroxyacetone derived N4-methyl substituted thiosemicarbazone: Syntheses, crystal structures and spectroscopic characterization of later first-row transition metal complexes, *J. Mol. Struct.*, 1224 (2021) 129055-129062.

[21] Santoro A., Vileno B., Palacios Ò., Díazd M.D.P., Riegel G., Gaiddon C., Krężel A., Faller P., Reactivity of Cu(II)-, Zn(II)- and Fe(II)- thiosemicarbazone complexes with glutathione and metallothionein: from stability to dissociation to transmetallation, *Metallomics*, 11 (2019) 994-1004.

[22] Cıkla I.K., Güveli S., Yavuz M., Demirci T.B., Ülküseven B., 5-Methyl-2-hydroxy-acetophenone-thiosemicarbazone and its nickel(II) complex: Crystallographic, spectroscopic (IR, NMR and UV) and DFT studies, *Polyhedron*, 105 (2016) 104-114.

[23] Sharma D., Jasinski J.P., Smolinski V.A., Kaur M., Paul K., Sharma R., Synthesis and structure of complexes (Ni^{II}, Ag^{I}) of substituted benzaldehyde thiosemicarbazones and antitubercular activity of NiII complex, *Inorg. Chim. Acta*, 499 (2020) 119187-119194.

[24] Konakanchi R., Haribabu J., Prashanth J., Nishtala V.B., Mallela R., Manchala S., Gandamalla D., Karvembu R., Reddy B.V., Yellu N.R., Kotha L.R., Synthesis, Structural, Biological Evaluation, Molecular Docking and DFT Studies of Co(II), Ni(II), Cu(II), Zn(II), Cd(II) and Hg(II) Complexes bearing Heterocyclic Thiosemicarbazone ligand, *Appl. Organomet. Chem.*, 32 (8) (2018) 4415.

[25] Arafath M.A., Adam F., Razali M.R., Hassan L.E.A., Ahamed M.B.K., Majid A.M.S.A., Synthesis, characterization and anticancer studies of Ni(II), Pd(II) and Pt(II) complexes with Schiff base derived from N-methylhydrazinecarbothioamide and 2-hydroxy-5-methoxy-3 nitrobenzaldehyde, *J. Mol. Struct.*, 1130 (2017) 791-798.

[26] Nyawade E.A., Sibuyi N.R.S., Meyer M., Lalancette R., Onani M.O., Synthesis, characterization and anticancer activity of new 2-acetyl-5-methyl thiophene and cinnamaldehyde thiosemicarbazones and their palladium(II) complexes, *Inorg. Chim. Acta*, 515 (2021) 20036-120045.

[27] Savir S., Wei Z.J., Liew J.W.K., Vythilingam I., Lim Y.A.L., Saad H.M., Sim K.S., Tan K.W., Synthesis, cytotoxicity and antimalarial activities of thiosemicarbazones and their nickel (II) complexes, *J. Mol. Struct.*, 1211 (2020) 128090-128099.

[28] Amuthakala S., Bharath S., Rahiman A.K., Thiosemicarbazone-based bifunctional chemosensors for simultaneous detection of inorganic cations and fluoride anion, *J. Mol. Struct.*, 1219 (2020) 128640-128654.

[29] Huseynova M., Farzaliyev V., Medjidov A., Aliyeva M., Taslimi P., Sahin O., Yalçın B., Novel zinc compound with thiosemicarbazone of glyoxylic acid: Synthesis, crystal structure, and bioactivity properties, *J. Mol. Struct.,* 1200 (2020) 127082-127091.

[30] Kalantari R., Asad Z., DNA/BSA binding of a new oxovanadium (IV) complex of glycylglycine derivative Schiff base ligand, *J. Mol. Struct.*, 1219 (2020) 128664-128675.

[31] Jacob J.M., Kurup M.R.P., Nisha K., Serdaroglu G., Kaya S., Mixed ligand copper(II) chelates derived from an O, N, S-donor tridentate thiosemicarbazone: Synthesis, spectral aspects, FMO and NBO analysis, *Polyhedron*, 189 (2020) 114736-114746.

[32] Li Q.X., Tang H.A., Li Y.Z., Wang M., Wang L.F., Xia C.G., Synthesis, characterization, and antibacterial activity of novel Mn(II), Co(II), Ni(II), Cu(II), and Zn(II) complexes with vitamin K3-thiosemicarbazone, *J. Inorg. Biochem.*, 78 (2) (2000) 167-174.

[33] Palve A.M., Garje S.S., Preparation of zinc sulfide nanocrystallites from single-molecule precursors, *J. Cryst. Growth*, 326 (1) (2011) 157-162.

[34] Attralarasan S., Febena A.S., Raj M.V.A, Madhavan J., Synthesis, Characterization and DFT Calculations ofnThiosemicarbazone 4-Methoxy Benzaldehyde Zinc Chloride, *Mechanics, Materials Science & Engineering,* 9 (2017).

[35] Kumar L.V., Sundaresan S., Gopinathan R.N., Antioxidant, antidiabetic and anticancer studies of nickel complex of Vanillin-4-Methyl-4-Phenyl-3-Thiosemicarbazone, *Mater. Today* 41 (3) (2021) 669-675.

[36] Ayyannan G., Mohanraj M., Gopiraman M., Uthayamalar R., Raja G., Bhuvanesh N., Nandhakumar R., Jayabalakrishnan C., New Palladium(II) complexes with ONO chelated hydrazone ligand: Synthesis, characterization, DNA/BSA interaction, antioxidant and cytotoxicity, *Inorg. Chim. Acta,* 512 (2020) 119868.

[37] Bashiri M., Jarrahpour A.S., Nabavizadeh M., Karimian S., Rastegari B., Haddadi E., Turos E., Potent antiproliferative active agents: novel bis Schiff bases and bis spiro β-lactams bearing isatin tethered with butylene and phenylene as spacer and DNA/BSA binding behavior as well as studying molecular docking, *Medic. Chem. Res.,* 30 (2021) 258–284.

[38] Amitha G.S., Vasudevan S., DNA binding and cleavage studies of novel Betti base substituted quaternary Cu(II) and Zn(II) phthalocyanines, *Polyhedron*, 190 (2020) 114773-114782.

[39] Husain M.A., Ishqi H.M., Sarwar T., Rehman S.U., Tabish M., Interaction of indomethacin with calf thymus DNA: a multi-spectroscopic, thermodynamic and molecular modelling approach, *Med. Chem. Comm.,* 8 (2017) 1283.

[40] Tian Z., Huang Y., Zhang Y., Song L., Qiao Y., Xu X., Wang C., Spectroscopic and molecular modeling methods to study the interaction between naphthalimide-polyamine conjugates and DNA, *J. Photochem. Photobiol. B.,* 158 (2016) 1–15.

[41] Mo D., Shi J., Zhao D., Zhang Y., Guan Y., Shen Y., Bian H., Huang F., Wu S., Synthesis and characterization of FeIII/CoIII/CuII complexes with Schiff base ligand and their hybrid proteins, SOD activity and asymmetric catalytic oxidation of sulfides, *J. Mol. Struct.*, 1223 (2021) 129229-129238.

[42] are W.R., Oxygen quenching of fluorescence in solution: an experimental study of the diffusion process, *J. Phys. Chem.,* 66 (3) (1962) 455–458.

[43] Singh R., Afzal M., Zaki M., Ahmad M., Tabassum S., Bharadwaj P.K., Synthesis, structure elucidation and DFT studies of a new coumarin-derived Zn(II) complex: in vitro DNA/HSA binding profile and pBR322 cleavage pathway, *RSC Adv.*, 4 (2014) 43504.

[44] Ambika S., Manojkumar Y., Arunachalam S., Gowdhami B., Sundaram K.K.M., Solomon R.V, Venuvanalingam P., Akbarsha M.A., Sundararaman M., Biomolecular Interaction, AntiNCancer and Anti-Angiogenic Properties of Cobalt(III) Schiff Base Complexes, *Sci. Rep.,* 9 (2019) 2721.

[45] Li Y., Yang Z., Li T., Synthesis, characterisation, in vitro DNA binding properties and antioxidant activities of Ln(III) complexes with chromone-3-carbaldehyde- (2′-hydroxy) benzoyl hydrazone, *Prog. React. Kinet. Mech.,* 40 (4) (2015) 313-329.

[46] Zhang Y.P., Li Y., Xu G.C., Li J.Y., Luo H.Y., Li J.Y., Zhang Li., Jia D.Z., Synthesis, crystal structure, DNA/bovine serum albümin binding and antitumor activity of two transition metal complexes with 4-acylpyrazolone derivative, *Appl. Organometal Chem.,* 33 (2019) 4668.

[47] Asadizadeha S., Amirnasra M., Tirani F.F., Mansouria A., Schenk K., DNA-BSA interaction, cytotoxicity and molecular docking of mononuclear zinc complexes with reductively cleaved N_2S_2 Schiff base ligands, *Inorganica Chimica Acta*, 483 (2018) 310–320.

[48] Narwane M., Dorairaj D.P., Chang Y.L, Karvembu R., Huang Y.H., Chang H.W., Hsu S.C.N., Tris-(2-pyridyl)-pyrazolyl Borate Zinc(II) Complexes: Synthesis, DNA/Protein Binding and In Vitro Cytotoxicity Studies, *Molecules*, 26 (2021) 7341.

[49] Liu J.J., Liu X.R., Zhao S.S., Yang Z.W., Yang Z., Syntheses, crystal structures, thermal stabilities, CT-DNA, and BSA binding characteristics of a new acylhydrazone and its Co(II), Cu(II), and Zn(II) complexes, *Journal Of Coordination Chemistry,* 73 (2020) 1159–1176.

[50] Amitha G.S., Vasudevan S., DNA/BSA binding studies of peripherally tetra substituted neutral azophenoxy zinc phthalocyanine, *Polyhedron*, 175 (2020) 114208.

[51] Bessegaa T., Chaves O.A., Martins F.M., Acunha T.V., Back D.F., Iglesias B.A., Oliveira G.M., Coordination of Zn(II), Pd(II) and Pt(II) with ligands derived from diformylpyridine and thiosemicarbazide: Synthesis, structural characterization, DNA/BSA binding properties and molecular docking analysis, *Inorganica Chimica Acta*, 496 (2019) 119049.

[52] Ramilo-Gomes F., Addis Y., Tekamo I., Cavaco I., Campos D., Pavan I.R., Gomes C.S.B., Brito V., Santos A.O., Domingues F., Luís A., Marques M.M., Pessoa J.C., Ferreira S., Silvestre S., Correia I., Antimicrobial and antitumor activity of S-methyl dithiocarbazate Schiff base zinc(II) complexes, *Journal of Inorganic Biochemistry*, 216 (2021) 111331.

[53] Daryanavard M., Jannesari Z., Javeri M., Abyar F., A new mononuclear zinc(II) complex: Crystal structure, DNA- and BSAbinding, and molecular modeling; in vitro cytotoxicity of the Zn(II) complex and its nanocomplex, *Spectrochimica Acta Part A: Molecular and Biomolecular Spectroscopy*, 233 (2020) 118175.

[54] Sakthi M., Ramu A., Synthesis, structure, DNA/BSA binding and antibacterial studies of NNO tridentate Schiff base metal complexes, *Journal of Molecular Structure*, 1149 (2017) 727-735.

[55] Gacki M., Kafarska K., Pietrzak A., Glowniak I.K., Wolf W.M., Synthesis, characterization, crystal structure and biological activity of metal(II) complexes with theophylline, *J. Saudi Chem. Soc.*, 23 (3) (2019) 346-354.

[56] Haribabu J., Sabapathi G., Tamizh M.M., Balachandran C., Bhuvanesh N.S.P., Venuvanalingam P., Karvembu R., Water-Soluble Mono- and Binuclear Ru(η6 -p-cymene) Complexes Containing Indole Thiosemicarbazones: Synthesis, DFT Modeling, Biomolecular Interactions, and In Vitro Anticancer Activity through Apoptosis, *Organomet,* 37 (8) (2018) 1242–1257.